© Universiti Tun Hussein Onn Malaysia Publisher's Office

JST

Journal of Science and Technology

Journal homepage: http://penerbit.uthm.edu.my/ojs/index.php/jst
ISSN : 2229-8460 e-ISSN : 2600-7924

Computational Study for Molecular Properties of Some of the Isolated Chemicals from Leaves Extract of *Guiera Senegalensis* as Aluminium Corrosion Inhibitor

A. M. Ayuba[1*], M. Abubakar[2]

[1]Department of Pure and Industrial Chemistry,
Faculty of Physical Sciences, Bayero University, Kano, NIGERIA

[2]Department of Science and Technology Education,
Faculty of Education. Bayero University, Kano, NIGERIA

*Corresponding Author

DOI: https://doi.org/10.30880/jst.2021.13.01.006
Received 05 March 2021; Accepted 12 May 2021; Available online 25 May 2021

Abstract: The present work describes the computational methods for the corrosion inhibition of aluminium using three selected chemical constituents (5-methyldihydroflavasperone, 5-methylflavasperone and methoxylated naphthyl butanone) reportedly obtained from the leaves extract of *Guirea senegalensis.* Quantum chemical calculations including E_{HOMO}, E_{LUMO}, energy gap (ΔE), electronegativity (χ), global hardness (η) and fraction of electrons transfer from the inhibitor molecule to the aluminium surface (ΔN) were calculated. The local reactive sites through Fukui indices which explain the effect of structural features of these components in relation to electrophilic and nucleophilic point of attack were evaluated. The similarities in quantum chemical parameters for the compounds obtained revealed that the adsorption strengths of the molecules will be mostly determined by molecular size rather than electronic structure parameters. Fukui indices showed that the point of interaction of inhibitor molecule with the Al(l10) surface were through aromatic carbon atom rich in pi-electrons and oxygen atom of the alkanone functional group in the inhibitor molecules. Molecular dynamics simulations describing the adsorption behavior of the inhibitor molecule on Al(110) surface through Forcite quench molecular dynamics were carried out. The compounds were found to all obey the mechanism of physical adsorption because of their relatively low adsorption energies.

Keywords: Computational, corrosion, aluminium, inhibition, *Guiera senegalensis*

1. Introduction

Corrosion is one of the major means through which metals deteriorate. Most metals get corroded when they are in contact with aggressive medium such as moisture in the air, acids, bases, salts, oils, aggressive metals polishes and liquid chemicals [1]. Also, when metals are exposed to gaseous materials such as formaldehyde, acid vapour and sulphur containing gases, they undergo corrosion [2]. Acids such as hydrochloric, hydrofluoric, phosphoric and nitric are used in industrial processes including pickling, etching and descaling of metals in industries, this normally results into corroding the metals involved [3-4]. Protection of metals and their alloys against corrosion when exposed to corrosive media or aggressive environment has attracted much attention globally as a result of huge losses of resources and finances that usually results annually [5].

Owing to its relative resistance to corrosion attack, lightweight, high strength, malleability, durability, ductility, conductivity and recyclability, aluminium is an exceptionally valuable metal. Aluminium and its alloys find extensive

*Corresponding author: ayubaabdullahi@buk.edu.ng

and large number of applications in different capacities at various industries including transportation, construction, packaging, and automobile, among others [6]. Presently, the corrosion inhibition of aluminum and its alloys are the subject of tremendous technological importance, because of their increased industrial applications [7]. Organic compounds containing heteroatoms or polar functional groups of nitrogen, oxygen and/or sulphur atoms in a conjugated system have been identified to exhibit good corrosion inhibiting properties as an alternative way of protecting metals from corrosion attack [8]. Inhibition by such compounds occur through the adsorption on the surface of the corroding metal and the efficiency of the inhibitor compound depends on the structural, chemical and mechanical characteristics of the adsorption layers of the metal under particular conditions [9].

Experimental methods are very useful means to explain the inhibition mechanism between the metal and inhibitor molecule. Nonetheless, they are often expensive and time consuming. Ongoing development in hardware and software computational tools has opened the ways for powerful use of computational chemistry in corrosion inhibition studies. Several quantum chemical methods and molecular modeling techniques have been applied to relate the inhibition performance of the inhibitors with their molecular properties [6]. Quantum chemical calculations have been broadly employed to study and understand the reaction mechanisms. Also, they have been confirmed to be a very powerful computational research tool in theoretical chemistry for investigating the corrosion inhibition of metals [10]. It has been shown that the effectiveness of inhibitor molecule in metals protection is related to its electronic and spatial molecular structure, relating the quantum chemical parameters and inhibition efficiency [11]. Theoretical parameters offer some major advantages in which the molecules and their various substituent and fragments can be directly characterized on the basis of their molecular structure only and the proposed mechanism of adsorption can be directly accounted for in terms of the chemical reactivity of the compounds under study [12]. In some circumstances the parameters connected with the electronic and chemical structure of the inhibitor molecule act concurrently on the inhibitor efficiency and may be difficult to decide which parameter plays the most important role in deciding the efficiency of the inhibitor [13]. This present work is aimed to study the performance of three selected compounds obtained from literature which are reportedly sourced from the leaves extract of *Guiera senegalensis* [14] which is to be used for the corrosion inhibition of aluminum Al(1 1 0) metal in gaseous phase. The experimental use of the extracts of *Guiera senegalensis* on aluminium in hydrochloric acid solution have also been reported elsewhere [3].

2. Methodology

The inhibiting action of *Guiera senegalensis* extract, like other natural product extracts, can be attributed to the adsorption of the phytochemical constituents on the aluminium metal surface. Accurate experimental determination of the contributions of the different constituents to the overall inhibiting effect is considerably hindered by the complex chemical compositions of its biomass extract. In the present work, the use of quantum chemical parameters and molecular dynamics simulations to highlight the individual contributions of some isolated compounds of *Guiera senegalensis* extract obtained from literature [14] was evaluated. Such calculations were performed to describe the electronic structures of some of the major chemical constituents of the leaves of *Guiera senegalensis*; 5-methyldihydroflavasperone, 5-methylflavasperone and Methoxylated naphthylbutanone with a view to establishing the active sites as well as local reactivity of the molecules. The simulations were performed by means of the density functional theory (DFT) electronic structure program DMol3 using a Mulliken population analysis. Electronic parameters for the simulation included restricted spin polarization using the DND basis set and the Perdew–Wang (PW) local correlation density functional. Local reactivity of the studied compounds was analysed by means of the Fukui indices (FI) to assess regions of nucleophilic and electrophilic behaviour. Other parameters such as global hardness (η) and softness (σ) which are being calculated according to Koopman's theory, from the values of E_{HOMO} and E_{LUMO} using equation, electronegativity (χ) and local softness s(r).

2.1 Sketching the Inhibitor Molecules and Geometry Optimization

Three inhibitor molecules of interest (5-methyldihydroflavasperone, 5-methylflavasperone and Methoxylated naphthylbutanone) [14] (Fig. 1) were sketched using Chemdraw Ultra 7.0 software. The sketched molecules were all subjected to geometry optimization in order to refine the geometry of their structures which also minimized their conformational and torsional energies. This job was carried out using the $DMol^3$ geometry optimization as contained in Accelrys Material Studio 7.0 software. The optimized structures were saved for further use in quantum calculations of some electronic and structural properties [15].

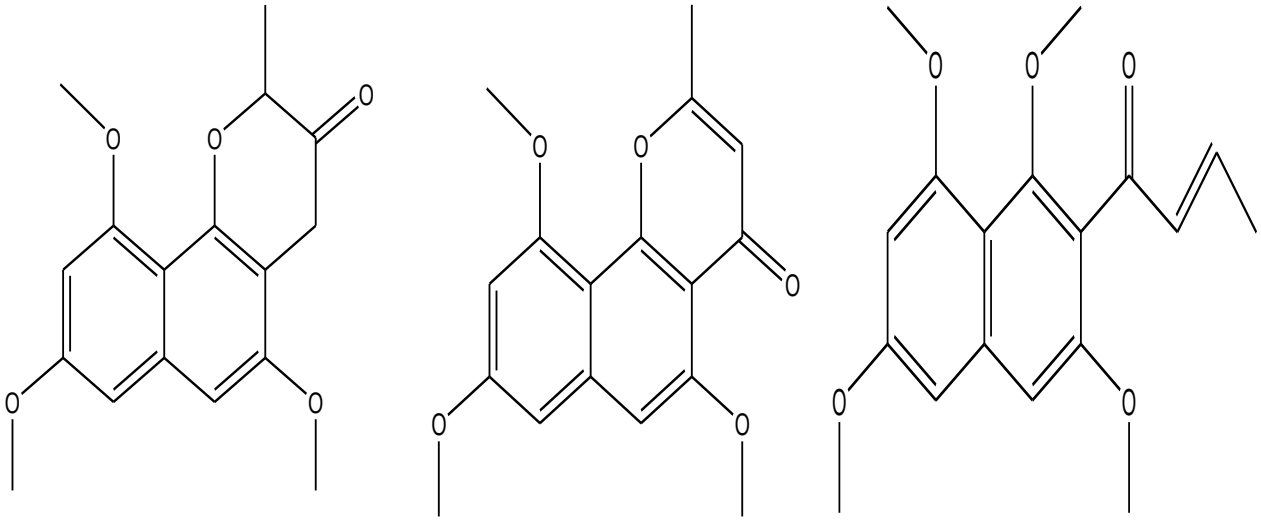

5,7,10-trimethoxy-3-methyl-3,4-dihydrophenanthren-2(1H)-one

5,7,10-trimethoxy-3-methylphenanthren-1(4H)-one

(2E)-1-(1,3,6,8-tetramethoxynaphthalen-2-yl)but-2-en-1-one

Fig. 1 - The sketched 2D structures of studied molecules

2.2 Quantum Chemical Calculations

Theoretical calculations were performed using the density functional theory (DFT) with B3YLP: 6-31G functional and DND as the basis set programs in DMol^3 as contained in the Materials Studio 7.0 software (Accelrys, Inc.). These calculations offer a very useful tool for understanding molecular properties and for describing the behavior of atoms in molecules [16]. They also provide an insight into chemical reactivity and selectivity, in terms of global reactivities such as global hardness (η), global softness (σ), frontier orbitals (HOMO and LUMO), electronegativity (χ) and local reactivity such as the Fukui function f(r) and local softness S(r) [17-19]. Ionization energy (I) and electron affinity (A) which are related to the energy of the highest occupied molecular orbital (E_{HOMO}) and lowest unoccupied molecular orbital (E_{LUMO}) and molecular weight of each molecule were all calculated using Eq. 1-4 [17, 20-22]:

$$\chi = \mu = -\left(\frac{\partial E}{\partial N}\right) v(r) \tag{1}$$

where μ is the chemical potential, its the negative of the electronegativity χ for N-electron system with total electronic energy E and an external potential $v(r)$, which has been defined as the first derivative of E with respect to N at constant external potential $v(r)$.

$$\eta = \left(\frac{\partial E^2}{\partial N^2}\right) v(r) = \left(\frac{\partial u}{\partial N}\right) v(r) \tag{2}$$

η is the global hardness which has been defined within the density functional theory (DFT) as the second derivative of energy E with respect to number of atoms N at constant $v(r)$.

$$I = -E_{HOMO} \tag{3}$$

$$I = -E_{HOMO} \tag{4}$$

Where I is the ionization potential and A is the electron affinity which are related in terms of energy of the highest occupied molecular orbital (E_{HOMO}) for ionization potential (I) and of the lowest unoccupied molecular orbital (E_{LUMO}) for electron affinity (A).

$$\chi = \frac{(I + A)}{2} = -\frac{E_{LUMO} + E_{HOMO}}{2} \tag{5}$$

$$\eta = \left(\frac{I - A}{2}\right) = -\frac{E_{LUMO} - E_{HOMO}}{2} \tag{6}$$

$$\sigma = {}^{1}/_{\eta} \quad (7)$$

Where χ is the electronegativity, η is the global hardness and σ is the Global softness.

Fraction of electrons transferred (ΔN) from the inhibitor molecule to the aluminium metal surface was calculated using the Eq. 8:

$$\Delta N = \frac{\chi Al - \chi inh}{2(\eta Al - \eta inh)} \quad (8)$$

where χAl = 5.6eV and χinh represents the absolute electronegativity of aluminium and the inhibitor molecule respectively. ηAl = 0 and ηinh stands for absolute global hardness of aluminium and the inhibitor molecule respectively.

The Fukui function f(r) is defined as the first derivative of the electronic density q(r) with respect to the number of electrons N at constant external potential v(r). This is achieved using a scheme of finite difference approximations from Mulliken population analysis of atoms for all the molecules under study. Calculations of point of nucleophilic attack $ƒ_K^+$ and electrophilic attack $ƒ_K^-$ were performed using Eq. 9-10 respectively as contained in the software.

$$ƒ_K^+ = q_K(N+1) - q_k(N) \quad (9)$$

$$ƒ_K^- = q_K(N) - q_k(N-1) \quad (10)$$

Where q_k is the gross charge of atom k in the molecule i.e the electron density at a point r in space around the molecule. N corresponds to the number of electrons in the molecule. *N + 1* corresponds to an anion, with an electron added to the LUMO of the neutral molecule, *N – 1* corresponds to the cation with an electron removed from the HOMO of the neutral molecule. All calculations were performed at the ground state geometry. These functions were condensed to the nuclei by using an atomic charge partitioning scheme, such as Mulliken and Hirshfeld model for population analysis.

2.3 Molecular Dynamics Simulation

Molecular Dynamics (MD) simulations were carried out at a molecular level using Forcite quench dynamics in order to sample many different low-energy configurations and find the low-energy minima for the best adsorption of each inhibitor molecule on the Al(1 1 0) metal surface as contained in the Materials Studio 7.0 software (Accelrys, Inc.) [6]. Computations were performed in a 5 x 4 supercell using the condensed-phase optimized molecular potentials for atomistic simulation studies (COMPASS) force field and the Smart algorithm in the software. Al(1 1 0) is the most densely packed and also the most stable among several types of Al surfaces [23-24]. The crystal of Al was cleaved along the (1 1 0) plane. The Al slab built for the docking process was relatively large enough to accommodate the inhibitor molecules in order to avoid edge effects during docking. Temperature was fixed at 350K, with NVE ensemble, time step of 1 fs and simulation time of 5 ps. The system was quenched every 250 steps with the Al(1 1 0) surface atoms constrained. The structures of the inhibitor molecule previously optimized were used for the simulation. Adsorption of a single inhibitor molecule onto the Al(1 1 0) surface offers access to the adsorption energetics and its effect on the inhibition efficiency of the molecule [24]. The binding energy (BE) or adsorption energy E_{ads}, between the inhibitor molecule and Al(1 1 0) surface was calculated using Eq. 11:

$$E_{ads} = -BE = E_{Al+Mol} - (E_{Al}) \quad (11)$$

where E_{ads} is the adsorption energy equal to negative of binding energy (*BE*), E_{Al+Mol} is the energy which corresponds to the total energies of Al(1 1 0) surface and the inhibitor molecule, E_{Mol} is the energy of the inhibitor molecule and E_{Al} is the energy of aluminium [24].

3. Results and Discussion

3.1 Quantum Chemical Calculations

Calculations were carried out in order to establish the active sites and local reactivity of all the three studied inhibitor molecules. Simulations were done by means of the DFT electronic structure program $DMol^3$ using a Mulliken population analysis [25-26]. Electronic parameters for the simulation include unrestricted spin polarization using the DND basis set and the Perdew–Wang (PW) local correlation density functional [6]. The result in Fig. 2-4 illustrate the (a) optimized structure, (b) electron density, (c) highest occupied molecular orbital (HOMO) and (d) lowest unoccupied molecular orbital (LUMO) of the studied inhibitor molecules A, B and C respectively. The optimized structure

represents the refined molecules that are brought to a stable geometry with a minimal torsional strength. The electron cloud in Fig. 2(b), 3(b) and 4(b) are saturated around each inhibitor molecule, the cloud of these electrons facilitate flat-lying adsorption orientations of inhibitor molecule onto Al(1 1 0) metal surface which is the most densely packed and also the most stable among several types of Al surfaces. In Fig. 2(c), 3(c) and 4(c), the regions of high HOMO density are the sites at which electrophiles attack and represent the active centers, with the utmost ability to bond to the metal surface. These regions of the HOMO orbitals are saturated on aromatic carbon atom containing the double bond (-C=C-) in the inhibitor molecules as presented. The LUMO orbital on the other hand (Fig. 2d, 3d, 4d), can accept free electrons in the p-orbital of the metal using antibonding orbitals to form feedback bonds [6, 27]. This can be observed to be applicable to all the studied molecules, for reason that they have a common base moiety qualifying a lot of structural and electronic similarities between them.

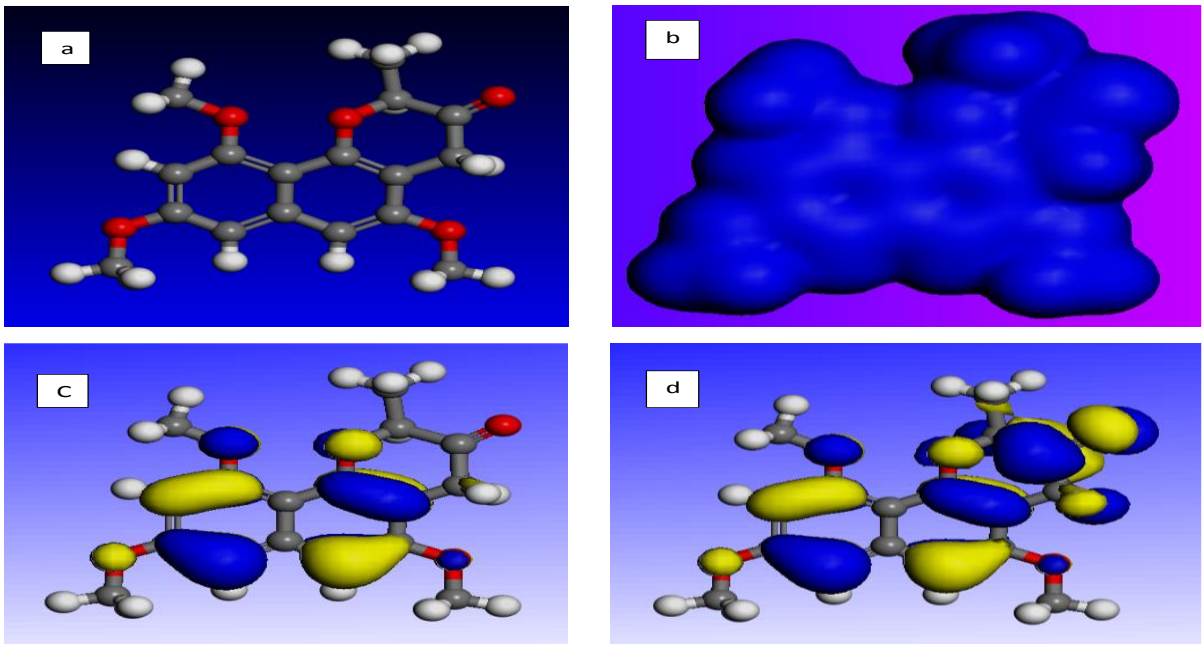

Fig. 2 - (a) Optimized structure; (b) Electron density around the optimized structure; (c) HOMO of the optimized structure; (d) LUMO of the optimized structure for molecule A

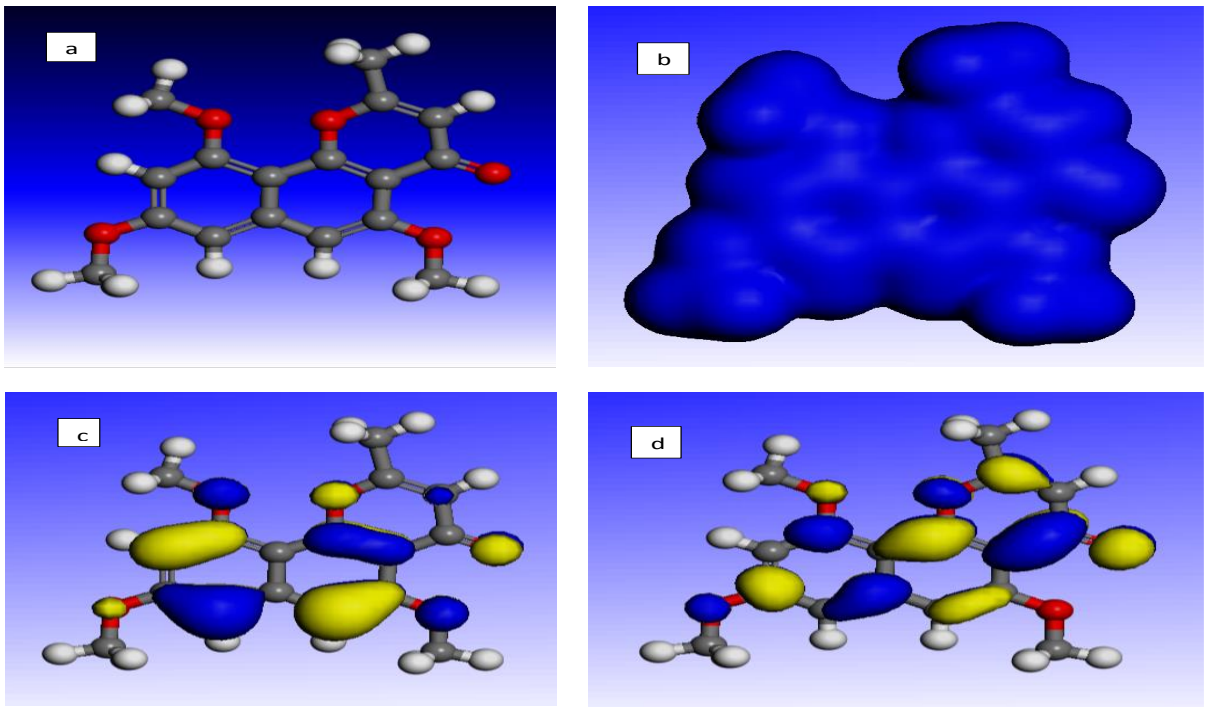

Fig. 3 - (a) Optimized structure; (b) Electron density around the optimized structure; (c) HOMO of the optimized structure; (d) LUMO of the optimized structure for molecule B

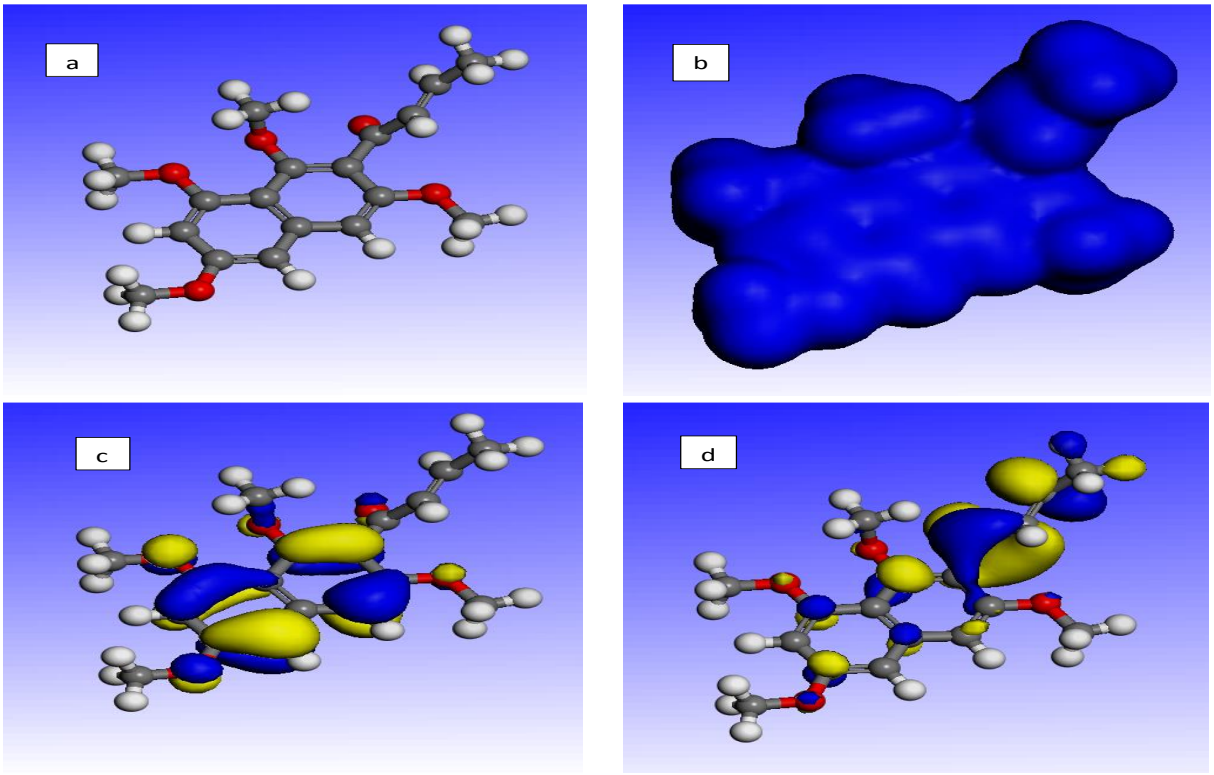

Fig. 4 - (a) Optimized structure; (b) Electron density around the optimized structure; (c) HOMO of the optimized structure; (d) LUMO of the optimized structure for molecule C

Table 1 presents the result of eigen values of highest occupied molecular orbital (E_{HOMO}) and lowest unoccupied molecular orbital (E_{LUMO}), the energy gap ΔE and other quantum chemical parameters. Highest E_{HOMO} (-5.355) was obtained with respect to molecule C, while lowest E_{HOMO} (-5.633) was obtained with respect to inhibitor B. High value of E_{HOMO} decreased the value of ΔE and high value of E_{LUMO} increased the value of ΔE, the smaller the energy gap between the HOMO and LUMO energy which is a function of reactivity, the stronger interaction of inhibitor molecule with the metal surface [28]. High values of E_{HOMO} indicate the disposition of the molecule to donate electrons to an appropriate acceptor like the unoccupied molecular orbital of the Al metal. Thus, a low ΔE value shows good inhibition efficiencies of the organic inhibitor because the energy to remove an electron from the last occupied orbital will be minimized [29-30]. The values of E_{HOMO} obtained show no significant difference between all the molecules which is due to the similarity of their molecular size containing the HOMO. The similarities in quantum chemical parameters mean that the adsorption strengths of the molecules will be mostly determined by molecular size parameters rather than electronic structure parameters [21]. Also, excellent organic inhibitors not only donate electrons to a vacant orbital of the metal, but they also accept free electrons from the metal which makes them more electron rich and therefore offer better inhibition efficiency. The result obtained in Table 1 shows that all the inhibitor molecules are rich in electrons since higher value of E_{LUMO} is an index that indicate the tendency of a molecular specie to accept free electron and offer good inhibition performance.

The values of fraction of fraction electron transferred from inhibitor molecule to the metal surface (ΔN) ranges from (0.493-0.563) with molecule B having the lowest value 0.493 and molecule C having the highest value 0.563 which are all less than 3.6. If ΔN is less than 3.6, inhibition efficiency increases with increase in values of the electron donating ability of the molecules while if the ΔN is greater than 3.6, the inhibition efficiency decreases with increasing values of the electron donating ability of the molecules [6]. The difference in electronegativity between the inhibitor molecules and aluminium drives the electron transfer. Therefore, all the three molecules inhibit the corrosion of aluminium in the following order of performance C<A<B with molecule B having the lowest ΔN value (0.493) because it has high capacity of donating more electrons leading to better inhibition performance [31].

Based on the result presented in Table 2, the electrophilic attack on inhibitor molecule A, B and C has their highest Mulliken and Hirshfeld charges each on C(3) of their structures. While for the nucleophilic attack, their highest Mulliken and Hirshfeld charges are on C(12), O(22) and O(21) for inhibitor molecule A, B and C respectively. All the C(3)'s are the carbon atoms containing the double bond (-C=C-) in aromatic ring of the inhibitor molecule A, B and C. C(12), O(22) and O(21) are the carbon and oxygen atom of ketone group of the inhibitor molecule A, B and C respectively. These are the region on the inhibitor molecules having the highest Mulliken and Hirshfield charges where the electrophilic and nucleophilic could possibly attack. The regions of a molecule where the Fukui function is large

are chemically softer than the regions where the Fukui function is small, and by invoking the HSAB principle in a local sense, one may establish the behavior of the different sites with respect to hard or soft reagents [20-21]. Thus all the molecules can accept and also release electrons mostly through the active centers specified by the Mulliken and Hirshfield model. This can clearly be observed on those centers on HOMO and the LUMO orbital in Fig. 2(c) – 4(c) and 2(d) – 4(d) respectively. The similarities in quantum chemical parameters mean that the adsorption strengths of the molecules will be mostly determined by molecular size parameters rather than electronic and/or structural parameters [6].

The values of Fukui indices for electrophilic (f^-) and nucleophilic (f^+) attack by Mulliken and Hirshfield model for inhibitor molecules A, B, and C respectively are presented in Table 2. The local reactivities of each molecule by means of Fukui indices indicates the regions of electrophilic and nucleophilic attack on the inhibitor molecules. f^- measure the ability of the molecule to release electrons or reactivities with respect to electrophilic attack, whereas f^+ measures the tendency of the molecule to attract electrons or reactivities relating to nucleophilic attack. Atom with highest Fukui value represents the point where electrophile or nucleophile can attack the molecule.

Table 1 - Quantum chemical parameters of the studied inhibitor molecules

Parameters	Inhibitor Molecules		
	A	**B**	**C**
HOMO (at orbital number)	80	79	84
LUMO (at Orbital number)	81	80	85
E_{HOMO} (eV)	-5.372	-5.633	-5.355
E_{LUMO} (eV)	-0.841	-1.183	-1.487
Energy gap (ΔE) (eV)	4.531	4.450	3.868
Molecular weight ($gmol^{-1}$)	302.326	300.310	316.353
Ionization potential (I) (eV)	5.372	5.633	5.355
Electron Affinity (A) (eV)	0.841	1.183	1.1487
Global hardness (η)	2.2655	2.2250	1.9340
Global softness (σ)	0.441	0.449	0.517
Absolute Electronegativity (χ)	3.107	3.408	3.421
Fraction of Electron Transfer (ΔN)	0.550	0.493	0.563

Key: A = 5-methyldihydroflavasperone B = 5-methylflavasperone C = methoxylated naphthyl butanone.

Table 2 - Calculated Fukui functions for all the inhibitor molecules (A-C)

Molecules	Electrophilic (F^-)		Nucleophilic (F^+)	
	Mulliken	**Hirshfeld**	**Mulliken**	**Hirshfeld**
A	(C3) 0.077	(C3) 0.088	(C12) 0.176	(O20) 0.163
B	(C3) 0.074	(C3) 0.083	(O22) 0.107	(O22) 0.104
C	(C3) 0.086	(C3) 0.101	(O21) 0.135	(O21) 0.129

Key: A = 5-methyldihydroflavasperone; B = 5-methylflavasperone; C = methoxylated naphthyl butanone.

3.2 Molecular Dynamic Simulation

Adsorption parameters for the interaction of the studied molecules with the Al(1 1 0) surface via Forcite quench dynamics were calculated. The total energies for the adsorption E_{ads} of inhibitor molecule A, B and C were computed by averaging the energies of the five most stable representative adsorption configurations which were presented in Table 3. The side view snapshot for the lowest energy adsorption configurations for single inhibitor molecules A, B and C, for the interaction with Al(1 1 0) surface were shown in Fig. 5(a), (b) and (c) respectively. The results shows that each inhibitor molecule maintained flat-lying adsorption orientation on the Al(1 1 0) metal surface, as shown by the delocalization of the electron density around all the molecules in Fig. 2(b), 3(b) and 4(b). This configuration maximizes contact between the molecule and the metal surface. It has been reported that, the more negative the E_{ads} of the inhibitor-metal surface, the better the adsorption of the inhibitor onto the metal surface and subsequently the higher the inhibition performance [32-33]. Based on the E_{ads} values obtained, molecule B having more negative value of E_{ads} is expected to perform better in inhibiting the corrosion of Al(1 1 0) in gas phase because of its molecular size and double bond on aromatic carbon atoms. This indicates that the larger molecules with electron donating ability are more strongly adsorbed on the metal surface. It can be observed from Table 3 that the magnitude of calculated E_{ads} values was all less than $100kcalmol^{-1}$, this is despite the fact that the simulations did not put into consideration the specific covalent interactions between the molecules and the Al(1 1 0) surface. Values less than or equal to $100kcalmol^{-1}$ have

been reported to be in the range of physical interactions [21, 33]. Therefore, adsorptions of these molecules on Al(1 1 0) surface in terms of their adsorption energy increases in the order of B>A>C. This observation is attributed to their molecular size and functional groups capable of donating electrons to the p-orbital of Al metal.

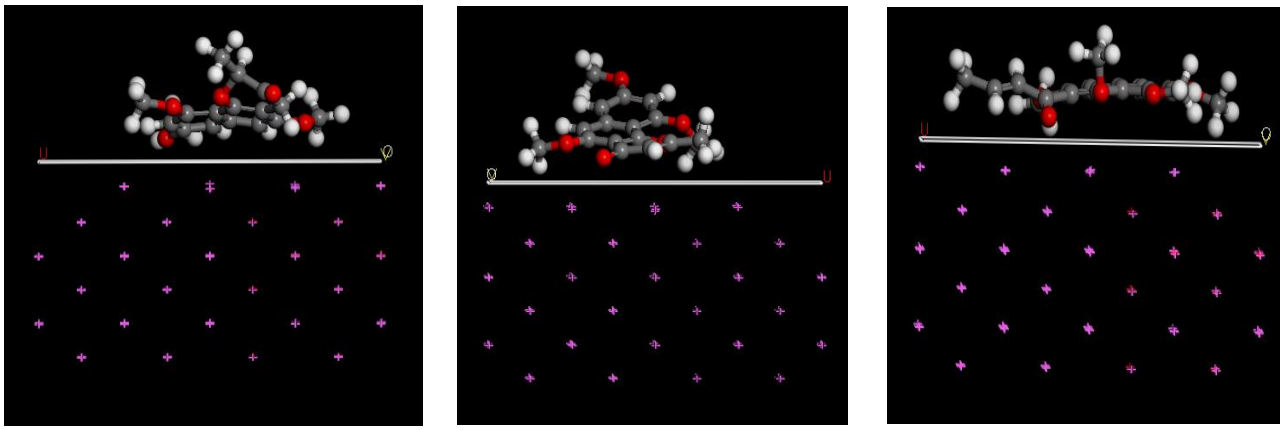

(a)-Molecule A (b)-Molecule B (c)-Molecule C

Fig. 5 - (a), (b) and (c) are the side view snap shots for the adsorption of inhibitor molecule A, B and C respectively on the Al(1 1 0) metal surface

Table 3 - Calculated adsorption parameters for the interaction of the inhibitor molecules (A, B and C) with the Al(1 1 0) surface

Molecule	Total Potential Energy (kcal/mol)	Molecular Energy (kcal/mol)	Energy of Al (1 1 0) surface (kcal/mol)	Adsorption Energy (kcal/mol)
A	-143.652±1.325	-71.571±2.554	0.000±000	-72.081±2.113
B	-136.417±5.389	-59.279±3.213	0.000±000	-77.138±3.812
C	-150.570±0.205	-81.122±1.221	0.000±000	-69.448±0.563

Key: A = 5-methyldihydroflavasperone; B = 5-methylflavasperone; C = Methoxylated naphthyl butanon

4. Conclusion

This work revealed that 5-methyldihydroflavasperone, 5-methylflavasperone and methoxylated naphthyl butanone reportedly sourced from *Guiera senegalensis* leaves extract inhibits the corrosion of Al(1 1 0). Quantum chemical parameters associated with the electronic structures of the inhibitor compounds and Fukui indices for electrophilic and nucleophilic attacks, indicated that the compounds could adsorb on the Al(1 1 0) surface through the aromatic carbon atoms containing the double bond and oxygen atoms from the ketone functional group. The molecular dynamics simulation results showed that all inhibitors have adsorption energies less than 100 $kcalmol^{-1}$ signifying a physical adsorption mechanism. The compounds were also established to be similarly adsorbed on the aluminum metal surface in the same flat lying pattern as indicated by the total electron density map of the compounds and the interaction of the carboxyl and methoxy functional groups of these compounds with the aluminium metal surface. This shows a great similarity in the structure of these three *Guiera senegalensis* selected compounds.

Acknowledgement

The contribution of Dr. Arthur David of Baze University, Abuja in installing the Acceryls Materials studio is highly acknowledged.

References

[1] Govindasamy, R., Ayappan, S. (2015). Study of Corrosion inhibition properties of novel Semicarbazones on mild steel in acidic solutions. Journal of the Chilean Chemical Society, 60, 2786–2798

[2] Ayuba, A. M., Abdullateef, A. (2020). Corrosion inhibition potentials of *Strichnos spinosa* L. on Aluminium in 0.9M HCl medium: experimental and theoretical investigations, Algerian Journal of Engineering and Technology, 03, 028–037

[3] Ayuba, A. M., Abubakar, M. (2021). Inhibiting aluminium acid corrosion using leaves extract of *Guiera senegalensis*, J. Fundam. Appl. Sci.13, 634–656

[4] Ladha, D. G., Wadhwani, P. M., Lone, M. Y., Jha, P. C., Shah, N. K. (2015). Evaluation of fennel seed extract as a green corrosion inhibitor for pure aluminum in hydrochloric acid: an experimental and computational approach. Analytical & Bioanalytical Electrochemistry, 7, 59–74
[5] Umaru, U., Ayuba, A. M. (2020). Quantum chemical calculations and molecular dynamic simulation studies on the corrosion inhibition of aluminium metal by myricetin derivatives, Journal of New Technology and Materials, 10, 18–28
[6] Ayuba, A. M., Uzairu, A., Abba, H., Shallangwa, G. A. (2018a). Hydroxycarboxylic acids as corrosion inhibitors on aluminium metal: a computational study. Journal of materials and environmental sciences, 9, 3026–3034
[7] Nyijime, T. A., Ayuba, A. M. (2020). Quantum chemical studies and molecular modeling of the effect of *coriandrum sativum l.* compounds as corrosion inhibitors on aluminum surface, Appl. J. Envir. Eng. Sci. 6, 344–355
[8] Douche, D., Elmsellem, H., Anouar, E. Guo, L., Hafez, B., Tuzun, B., El Louzi, A., Bougrin, K., Karrouchi, K., Himmi, B. (2020). Anti-corrosion performance of 8-hydroxyquinoline derivatives for mild steel in acidic medium: Gravimetric, electrochemical, DFT and molecular dynamics simulation investigations, Journal of Molecular liquids, 308, 113042
[9] Verma, C., Saji, V. S., Quraishi, M. A., Ebenso, E. E. (2020). Pyrazole derivatives as environmental benign acid corrosion inhibitors for mild steel: Experimental and computational studies, Journal ofMolecular Liquids, 298, 111943
[10] Hadisaputra, S., Purwoko, A. A., Savalas, L. R. T., Prasetyo, N., Yuanita, E., Hamdiani, S. (2020). Quantum chemical and monte carlo simulation studies on inhibition performance of caffeine and its derivatives against corrosion of copper, Coatings, 10, 1086
[11] Ayuba, A. M., Abdullateef, A. (2021). Investigating the corrosion inhibition potentials of *Strichnos spinosa l.* Extract on aluminium in 0.3M hydrochloric acid solution, J. Appl. Sci. Envir. Stud., 4, 336–348
[12] Hsissou, R., Benhiba, F., About, S., Dagdag, O., Benkhaya, S., Berisha, A., Erramli, H. (2020). Trifunctional epoxy polymer as corrosion inhibition material for carbon steel in 1.0 M HCl: MD simulations, DFT and complexation computations, Inorganic Chemistry Communications, 115, 107858
[13] Ammouchi, N., Allal, H., Belhocine, Y., Bettaz, S., Zouaoui, E. (2020). DFT computations and molecular dynamics investigations on conformers of some pyrazinamide derivatives as corrosion inhibitors for aluminium, Journal of molecular liquids, 300, 12309
[14] Silva, O., Gomez, E. T. (2003). Guieranone A, a naphtyl butenone from the leaves of Guiera senegalensis with antifungal activity, J. Nat. Prod., 66, 447–449
[15] Ayuba, A. M., Nyijime, T. A., Muhammad, A. S. (2020). Density functional theory and molecular dynamic simulation studies on the corrosion inhibition of some thiosemicarbazide derivatives on aluminum metal, Journal of Applied Surfaces and Interfaces, 8, 7–14
[16] Obot, I., Obi-Egbedi, N., Ebenso, E., Afolabi, A., Oguzie, E. (2013). Experimental, quantum chemical calculations, and molecular dynamic simulations insight into the corrosion inhibition properties of 2-(6-methylpyridin-2-yl) oxazolo [5, 4-f][1, 10] phenanthroline on mild steel. Research on Chemical Intermediates, 39, 1927–1958
[17] Eddy, N. O., Ameh, P. O., Essien, N. B. (2018). Experimental and computational chemistry studies on the inhibition of aluminium and mild steel in 0.1 M HCl by 3-nitrobenzoic acid. Journal of Taibah University for Science, 12, 545–556
[18] Kumar, A., Shukla, R., Venkatachalam, A. (2013). Studies of corrosion and electrochemical behavior of some metals and brass alloy under different media. Rasayan J. Chem, 6, 12–14
[19] Salman, T.A., Al-Azawi, K.F., Mohammed, I.M., Al-Baghdadi, S.B., Al-Amiery, A.A., Gaaz, T.S., Kadhum, A. A. (2018). Results in Physics, 10, 291–296
[20] Sundari, C., Setiadji, S., Ramdhani, M. A., Ivansyah, A., Widhiasari, N. (2018). Additional halogen group (F, Cl, and Br) to 2-Phenyl-imidazole [1, 2α] pyridine on corrosion inhibition properties: a computational study. Mater. Sci. Eng, 288, 012033
[21] Ayuba, A. M., Uzairu, A., Abba, H., Shallangwa, G. A. (2018b). Theoretical study of aspartic and glutamic acids as corrosion inhibitors on aluminium metal surface. Moroccan Journal of Chemistry, 6, 2160–2172
[22] Lgaz, H., Salghi, R., Chaouiki, A., Shubhalaxmi, S. Jodeh, S., Bhat, K. S. (2018). Pyrazoline derivatives as possible corrosion inhibitors for mild steel in acidic media: A combined experimental and theoretical approach. Cogent Engineering, 51441585
[23] Zhao, H., Zhang, X., Ji, L., Hu, H., Li, Q. (2014). Quantitative structure-activity relationship model for amino acids as corrosion inhibitors based on the support vector machine and molecular design. Corrosion Science, 83, 261–271
[24] Mishra, A., Verma, C., Srivastava, V., Lgaz, H., Quraishi, M.A., Ebenso, E. E., Chung, M. (2018). Chemical, electrochemical and computational studies of newly synthesized novel and environmental friendly heterocyclic compouds as corrosion inhibitors for mild steel in acidic medium. Journal of Bio- and Tribo-Corrosion, 4, 32

[25] Delley, B. (1990). An all-electron numerical method for solving the local density functional for polyatomic molecules. The Journal of chemical physics, 92, 508–517
[26] Delley, B. (2000). From molecules to solids with the $DMol^3$ approach. The Journal of chemical physics, 113, 7756–7764
[27] Shehu, N. U., Gaya, U. I., Muhammad, A. A. (2019). Influence of side chain on the inhibition of aluminium corrosion in HCl by α-amino acids, Applied Science and Engineering Progress, 12, 186–197
[28] Nazir, U., Akhter, Z., Janjua, N. K., Asghar, M. A., Kanwal, S., Butt, T. M., Sani, A., Liaqat, F., Hussain, R., Shah, F. U. (2020). Biferrocenyl Schiff bases as efficient corrosion inhibitors for an aluminium alloy in HCl solution: a combined experimental and theoretical study, RSC Adv., 10, 7585–7599
[29] Bashir, S., Thakur, A., Lgaz, H., Chung, I., Kumar, A. (2020). Corrosion inhibition efficiency of bronopol on aluminium in 0.5 M HCl solution: Insights from experimental and quantum chemical studies, Surfaces and interphases, 20, 100542
[30] Ayuba, A. M., Auta, M. A., Shehu, N. U. (2020). Comparative study of the inhibitive properties of ethanolic extract of *Gmelina arborea*on corrosion of aluminium in different media, Appl. J. Envir. Eng. Sci., 6, 374–386
[31] Umar, U., Muhammad, A. A. (2020). Computational study of anticorrosive effects of some thiazole derivatives against the corrosion of aluminium, RHAZES: Green and Applied Chemistry. 10, 113–128
[32] Awe, F. E., Idris, S. O., Abdulwahab, M., Oguzie, E. E. (2015). Theoretical and experimental inhibitive properties of mild steel in HCl by ethanolic extract of *Boscia senegalensis*. Cogent Chemistry, 1, 1112676
[33] John, S., Joseph, A. (2013). Quantum chemical and electrochemical studies on the corrosion inhibition of aluminium in 1N HNO_3 using 1, 2, 4-triazine. Materials and Corrosion, 64, 625–632